

# Bio-mimicking rotary nanomotors

Anatoly Smirnov<sup>a,b</sup>, Lev Mourokh<sup>c\*</sup>, Sergei Savel'ev<sup>a,d</sup>, Franco Nori<sup>a,b</sup>

<sup>a</sup>Advanced Science Institute, The Institute of Physical and Chemical Research (RIKEN),  
Wako-shi, Saitama, 351-0198, Japan;

<sup>b</sup>Center for Theoretical Physics, Physics Department, The University of Michigan, Ann Arbor, MI  
48109-1040, USA;

<sup>c</sup>Department of Physics, Queens College, The City University of New York, Flushing, New York  
11367, USA;

<sup>d</sup>Department of Physics, Loughborough University, Loughborough LE11 3TU, UK

## ABSTRACT

We propose a simple design of a rotary nanomotor comprised of three quantum dots attached to the rotating ring (rotor) in the presence of an in-plane dc electric field. The quantum dots (sites) can be coupled to or decoupled from source and drain carrier reservoirs, depending on the relative positions of the leads and the dots. We derive equations for the site populations and solve these equations numerically jointly with the Langevin-type equation for the rotational angle. It is shown that the synchronous loading and unloading of the sites results in unidirectional rotation of the nanomotor. The corresponding particle current, torque, and energy conversion efficiency are determined. Our studies are applicable both to biologically-inspired rotary nanomotors, the  $F_0$  motor of ATP synthase and the bacterial flagellar motor, which use protons as carriers, and to novel artificial semiconductor systems using electrons. The efficiency of this semiconductor analog of the rotary biomotors is up to 85% at room temperature.

**Keywords:** nanomotor, rotary motors, electron tunneling, rate equations

## 1. INTRODUCTION

Biological rotary motors provide remarkable examples of how electrochemical energy can be efficiently converted into mechanical motion [1, 2]. Two of the most important representatives of this family, the  $F_0$  motor of ATP (adenosine triphosphate) synthase and the bacterial flagellar motor, are powered by  $H^+$  or  $Na^+$  ions, which flow down the electrochemical gradient across the mitochondrial or cell membranes, thereby generating a torque [3-6]. Both of these rotary motors have similar components: (i) a stator, tightly attached to the membrane, and (ii) a ring-shaped rotor, which can freely rotate around its axis. It is assumed [3-5] that the rotor has several (10 to 14) proton-binding sites. In the presence of an external electric field (which might be created by the charges stored in the stator), the population of these sites by charged particles (protons) can lead to a rotational torque.

In this paper we propose a simple model of an *electronic* device based on the same principles. In some sense, the structure of such artificial system can be even simpler than that of the original biological one (see Fig. 1). Three quantum dots (mimicking protonable sites) can be attached (or embedded) to the rotating rings. Electron states in these dots are tunnel-coupled to two reservoirs (source and drain) allowing the population and depopulation of the dots. We show below that the second source reservoir allows us to alternate the direction of rotation. This electronic counterpart of biological motors can be placed in an external electric field (in particular, inside a capacitor) thereby inducing a torque.

We examine the dynamics of this bio-mimicking nanomotor using methods of condensed matter physics which are natural for this case and have been successful for the modeling of real biological motors. In our previous publications [7,8], we used them to describe the loading/unloading of protonable sites in the  $F_0$  motor of ATP-synthase. (Afterwards, the same idea was used for the electron-tunneling-powered rotation of the “blade-nanotube” structure [9].) In the present paper, our Hamiltonian includes the mechanical part describing the nanomotor rotation with the kinetic term and heat bath term responsible for friction; transfer Hamiltonian for electron tunneling between reservoirs and the dots; inter-dot

---

\* lev.murokh@qc.cuny.edu; phone 1 718 997-4893; fax 1 718 997-3349

Coulomb interaction; and coupling of the electrons to an external electric field. We introduce possible electronic states in the system and derive a master equation for their density matrix. This equation is coupled to the Langevin equation for the rotating angle. A numerical solution of these equations allows us to describe the rotation of the nanomotor, determine the time evolution of the dot populations and induced torque, as well as obtain the dependencies of the time-averaged torque and electron particle current on the source-drain voltage, in-plane electric field, and temperature. Of special interest is the system behavior in the presence of an external torque. We show that if this torque is large enough, the nanomotor can work in the *reverse regime*, pumping electrons against the applied voltage.

## 2. MODEL

The system under consideration here consists of three equally-spaced quantum dots A, B, and C attached to the rotating ring (rotor) in the presence of a constant  $y$ -directed electric field (Fig.1). The dots can be coupled to two electron sources  $S_1$  and  $S_2$  as well as to the electron drain  $D$ . The source leads  $S_1$  and  $S_2$  can be connected (or disconnected) at will to the electron reservoir with an electrochemical potential  $\mu_S$ , whereas the drain is connected to the reservoir with the electrochemical potential  $\mu_D$  smaller than  $\mu_S$ . We show below that the activation of the lead  $S_1$  results in a clockwise motion of the rotor, whereas a connection of the  $S_2$ -lead (and disconnection of the  $S_1$ -lead) generates a counterclockwise rotation. At each instant of time only one source lead is connected to the reservoir.

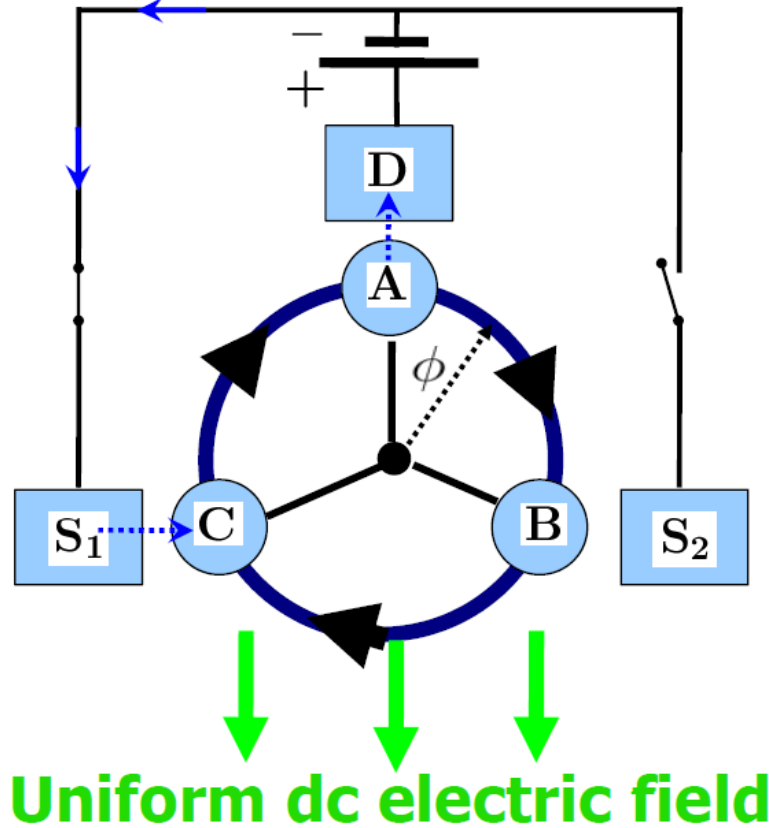


Fig. 1. Schematics of the nanomotor. With  $S_1$ -lead connected to the circuit, the rotor experiences the clockwise rotation.

The Hamiltonian of the system has the form:

$$H = \frac{p^2}{2Mr_0^2} - U_0 \sum_{\sigma} n_{\sigma} \cos(\phi + \phi_{\sigma}) + \sum_{\sigma} E_{\sigma} n_{\sigma} + \sum_{k,\alpha} E_{k\alpha} c_{k\alpha}^{\dagger} c_{k\alpha} + \sum_{\sigma,\sigma'} U_{\sigma\sigma'} n_{\sigma} n_{\sigma'} + H_{tun} + H_Q, \quad (1)$$

where  $\phi$  is the angle of rotation,  $p = -i\hbar(\partial/\partial\phi)$  is the operator of angular momentum of the rotator with radius  $r_0$  and effective mass  $M$ . We take into account here the effects of a constant  $y$ -directed external electric field, with a potential energy profile

$$U(\phi) = -U_0 \cos \phi,$$

on the electrons localized in the three sites  $\sigma = A, B, C$  with positions, characterized by the angles  $\phi_A, \phi_B, \phi_C$ , respectively. The operators  $a_\sigma^+$  and  $a_\sigma$  describe the creation and annihilation of an electron on the site (dot)  $\sigma$  with a population  $n_\sigma = a_\sigma^+ a_\sigma$ , whereas the operators  $c_{k\alpha}^+$  and  $c_{k\alpha}$  are related to the  $k$ -state of the electron in the source and drain reservoirs (leads) with energy  $E_{k\alpha}$  ( $\alpha = S_1, S_2, D$ ). The Coulomb repulsion between electrons is given by the potentials  $U_{\sigma\sigma}$ . The tunneling coupling between dots and leads is given by the Hamiltonian

$$H_{tun} = \sum_{k,\alpha,\sigma} T_{k\alpha} c_{k\alpha}^+ a_\sigma w_{\alpha\sigma}(\phi) + h.c., \quad (2)$$

where the tunneling amplitudes  $T_{k\alpha}$  are multiplied by the factor

$$w_{\alpha\sigma}(\phi) = \exp\left[-\frac{\sqrt{2}r_0}{\lambda} \sqrt{1 - \cos(\phi + \phi_\sigma - \phi_\alpha)}\right], \quad (3)$$

which reflects an exponential dependence of the tunneling rate on the distance between the  $\sigma$ -dot and the  $\alpha$ -lead with a characteristic spatial scale  $\lambda$ . To take into account the influence of the classical dissipative environment  $\{Q\}$  with the Hamiltonian  $H_{Bath}$  on the rotational degrees of freedom, we include the term

$$H_Q = -r_0 \phi Q + H_{Bath}$$

in Eq. (1). Correspondingly, the nanorotator experiences Brownian motion by the Langevin equation in the overdamped regime

$$\zeta \dot{\phi} + U_0 \sum_{\sigma} n_{\sigma} \sin(\phi + \phi_{\sigma}) = \xi + N_{ext}, \quad (4)$$

where  $\zeta = 4\pi\eta r_0^2 h$  is the drag coefficient,  $N_{ext}$  is the external torque acting on the nanomotor,  $\eta$  is the viscosity,  $h$  is the nanomotor height, and the Gaussian fluctuation source  $\xi$  is characterized by the correlation function:  $\langle \xi(t)\xi(t') \rangle = 2\zeta T \delta(t-t')$ .

To describe the process of loading and unloading of proton-binding sites A, B, and C, we introduce the electron vacuum state

$$|1\rangle = |\text{vacuum}\rangle,$$

jointly with seven additional states,

$$|2\rangle = a_A^+ |1\rangle,$$

$$|3\rangle = a_B^+ |1\rangle,$$

$$|4\rangle = a_A^+ a_B^+ |1\rangle,$$

$$|5\rangle = a_C^+ |1\rangle,$$

$$|6\rangle = a_A^+ a_C^+ |1\rangle,$$

$$|7\rangle = a_B^+ a_C^+ |1\rangle,$$

$$|8\rangle = a_A^+ a_B^+ a_C^+ |1\rangle.$$

Each of the electron operators can be expressed in terms of the operators  $\rho_{\mu\nu} = |\mu\rangle\langle\nu|$  ( $\mu, \nu = 1, \dots, 8$ ). The populations of the dots,  $n_\sigma$ , are expressed in terms of the diagonal operators  $\rho_\mu \equiv \rho_{\mu\mu}$ , as:

$$n_A = \rho_2 + \rho_4 + \rho_6 + \rho_8,$$

$$n_B = \rho_3 + \rho_4 + \rho_7 + \rho_8,$$

$$n_C = \rho_5 + \rho_6 + \rho_7 + \rho_8.$$

Thus, for the electrons localized on the rotor sites  $A, B, C$  we obtain the Hamiltonian

$$H_{ABC} = \sum_{\mu=1}^8 \varepsilon_\mu |\mu\rangle\langle\mu|,$$

with an energy spectrum depending on the local value of the rotor angle  $\phi$ .

$$\varepsilon_1 = 0,$$

$$\varepsilon_2 = E_A - U_0 \cos(\phi + \phi_A),$$

$$\varepsilon_3 = E_B - U_0 \cos(\phi + \phi_B),$$

$$\varepsilon_4 = \varepsilon_2 + \varepsilon_3,$$

$$\varepsilon_5 = E_C - U_0 \cos(\phi + \phi_C),$$

$$\varepsilon_6 = \varepsilon_2 + \varepsilon_5,$$

$$\varepsilon_7 = \varepsilon_3 + \varepsilon_5,$$

$$\varepsilon_8 = \varepsilon_2 + \varepsilon_3 + \varepsilon_5.$$

We assume here that the characteristic time,  $\gamma^{-1}$ , of electron tunneling to and out of the dots is much shorter than the time scale of the rotary angle,  $\langle \dot{\phi} \rangle$ , and that the noise produced by the electron tunneling between the dots and the source and drain contacts has much less effect on the mechanical motion of the rotor than the noise  $\zeta$  generated by the bath  $\{Q\}$ . Accordingly, we can average the stochastic Eq. (4) over fluctuations of the electron reservoirs without averaging over the fluctuations of the mechanical heat bath. The partially averaged proton population  $n_\sigma$  involved in Eq. (4) depends on the local fluctuating value of the rotational angle  $\phi$ . To determine these populations, we derive the following master equation for the proton distribution  $\rho_\mu$ , averaged over reservoirs fluctuations,

$$\dot{\rho}_\mu + \gamma_\mu \rho_\mu = \sum_\nu \gamma_{\mu\nu} \rho_\nu, \quad (5)$$

with

$$\gamma_{\mu\nu} = \sum_{\alpha, \sigma} \Gamma_\alpha(\phi) \left\{ |a_{\sigma, \mu\nu}|^2 \left( 1 - f_\alpha(\omega_{\nu\mu}) \right) + |a_{\sigma, \nu\mu}|^2 f_\alpha(\omega_{\mu\nu}) \right\}, \quad (6)$$

$\gamma_\mu = \sum_\nu \gamma_{\mu\nu}$ , and  $\Gamma_\alpha(\phi) = \Gamma_\alpha |w_{\alpha\alpha}(\phi)|^2$ ,  $\omega_{\nu\mu} = \varepsilon_\mu - \varepsilon_\nu$  ( $\hbar = 1$ ),  $\Gamma_\alpha = 2\pi \sum_k |T_{k\alpha}|^2 \delta(\omega - \omega_{\nu\mu})$  [10,11], and  $a_{\sigma, \mu\nu}$  are the matrix elements of corresponding annihilation operators. The electrons in the reservoirs are characterized by the Fermi distributions,  $f_\alpha(\omega) = [\exp\{(\omega - \mu_\alpha)/T\} + 1]^{-1}$  with electrochemical potentials  $\mu_S = V/2$ ,  $\mu_D = -V/2$ , where  $V$  is the electron voltage applied to the system and  $T$  is the temperature ( $k_B = 1$ ). We include the absolute value of the electron charge,  $|e|$ , into the definition of the voltage  $V$  and measure the voltage in units of energy, meV. Notice that, despite of the averaging over electron reservoirs, the master equation, Eq. (5), contains a stochastic component, which is determined by the fluctuations of the rotor angle  $\phi(t)$ , taken at the same time  $t$ . Eq. (5) is valid for weak coupling between dots and leads, and for the case when the angular coordinate  $\phi(t)$  does not change significantly on the characteristic time scale,  $\tau_T = \pi/T$ , of the Fermi distribution.

The solution of the master equation, Eq. (5), jointly with the Langevin equation, Eq. (4), allows us to determine the average electron particle current through the structure, defined as

$$I = -I_S = -\frac{d}{dt} \sum_k \langle c_{kS}^+ c_{kS} \rangle \quad (7)$$

for any of two sources which can be connected to the nanomotor, as well as the torque induced in the system

$$N = -\sum_{\sigma} \left\langle n_{\sigma} \frac{dU(\phi + \phi_{\sigma})}{d\phi} \right\rangle. \quad (8)$$

### 3. NUMERICAL RESULTS

We consider here the rotation of a system with height  $h = 10$  nm and radius  $r_0 = 100$  nm. Three torque-generating sites, A, B, and C, are attached at the points  $\phi_A = 0$ ,  $\phi_B = 2\pi/3$ , and  $\phi_C = -2\pi/3$ , respectively. The locations of the two possible source contacts  $S_1, S_2$  and the drain  $D$  are defined by  $\phi_{S1} = -2\pi/3$ ,  $\phi_{S2} = 2\pi/3$ ,  $\phi_D = 0$ . For the Coulomb interaction between sites in a medium with a dielectric constant  $\epsilon_r \sim 7$ , we obtain:  $U_{ab} \simeq U_{bc} \simeq U_{ac} \simeq 1.15$  meV. We choose the value  $10^{-3}$  Pa·s for the viscosity assuming a water environment for the nanomotor.

In Fig. 2, we present a summary of our numerical solution of the Langevin equation coupled to the master equation, for the source-drain voltage  $V = \mu_S - \mu_D = 500$  meV, external potential  $U_0 = 200$  meV, the tunneling couplings to the leads  $\Gamma_S = \Gamma_D = 2 \cdot 10^5$  s<sup>-1</sup>, electron tunneling length  $\lambda = 1$  nm, and temperature  $T = 300$  K when the source contact  $S_1$  is activated, the rotor moves in the clockwise (positive) direction. Switching on the source contact  $S_2$  leads to the same behavior, but with a rotation in the counterclockwise (negative) direction.

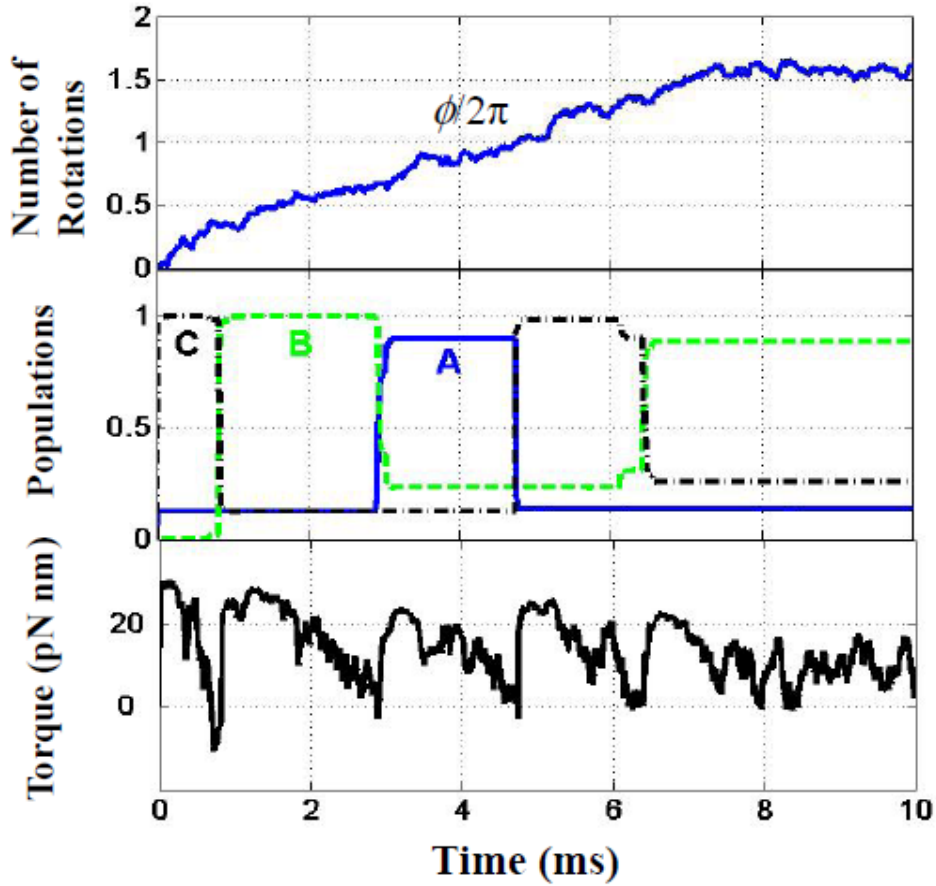


Fig. 2. Time evolution of (a) the rotational angle, (b) populations of the dots, and (c) the induced torque.

It is evident from Fig. 2 that successive populations and depopulations of the dots lead to a continuous nanomotor rotation and for this set of parameters the full rotation occurs for about 4.8 s. The torque changes from zero (or even negative values due to thermal fluctuations) to more than 20 pN-nm.

Fig. 3 illustrates the synchronous dynamics of loading and unloading the dots A, B, and C having populations  $n_A$ ,  $n_B$ , and  $n_C$ , when they pass through the source and the drain leads.

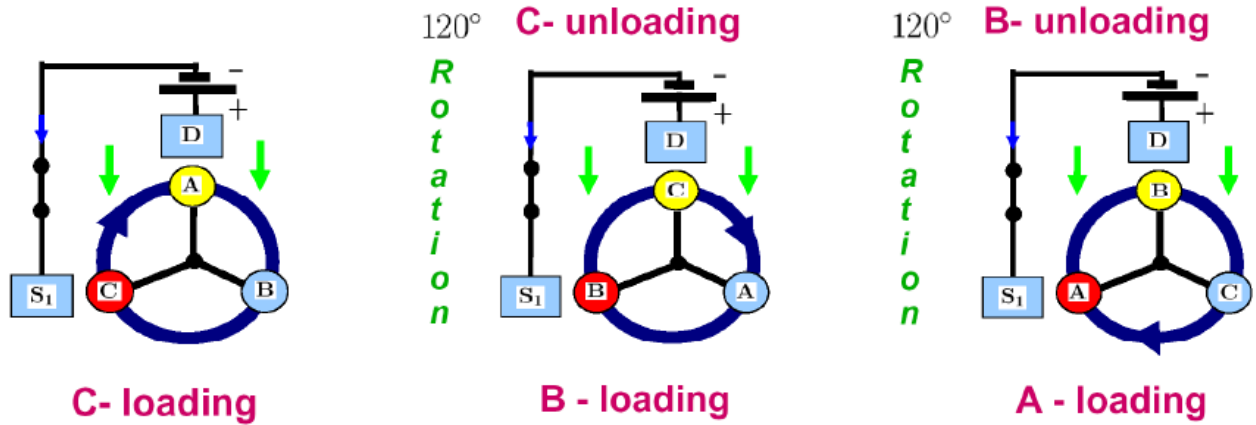


Fig. 3. Subsequent populations and depopulations of the three dots.

The site  $C$  is populated first because of its close proximity to the source lead  $S_1$ . The external electric field pushes the  $C$ -electron, and, correspondingly, the whole rotor unit, to turn through the angle  $2\pi/3$  to the position of the minimum of the potential  $U = -U_0 \cos(\phi + \phi_C)$ . At this position of the rotor, the site  $C$  approaches the drain contact  $D$  and unloads the electron. At the same rotor position, the site  $B$  starts to be populated since this site is in the loading range of the source lead  $S_1$ . This leads to a subsequent  $120^\circ$ -turn of the rotor. This process repeats over and over, resulting in a continuous unidirectional rotation of the rotary ring.

The dependence of the average particle current on the applied source-drain voltage is shown in Fig. 4 for various temperatures.

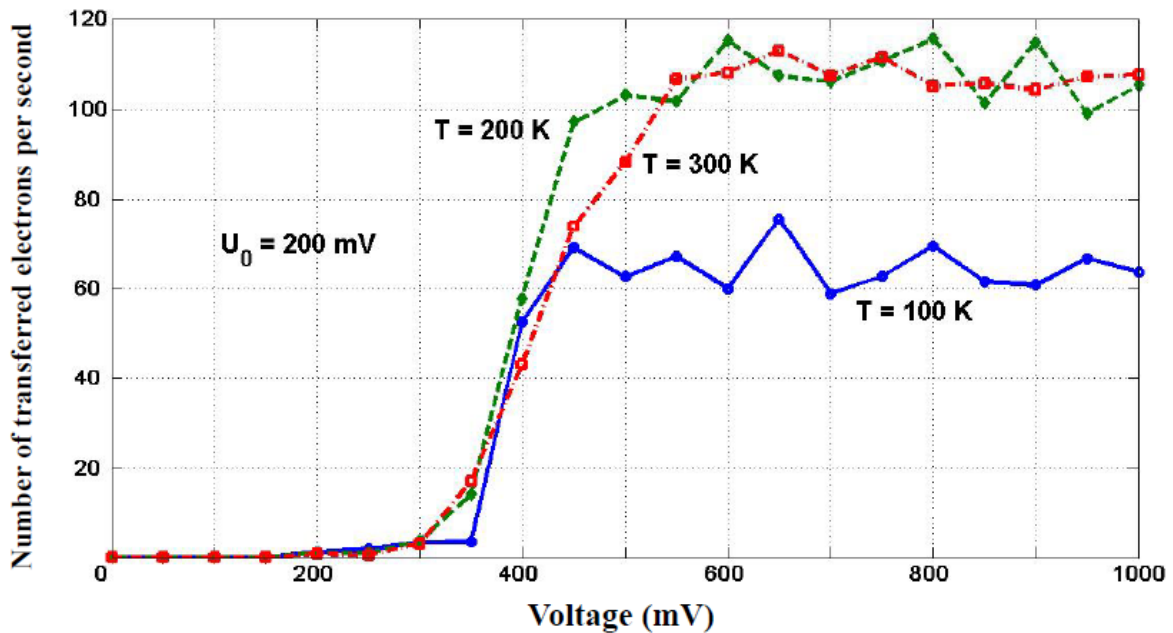


Fig. 4. Average electron particle current as a function of the source-drain voltage.

One can see that voltages smaller than 350 mV are not enough to overcome the friction and produce charge transport and, consequently, the nanomotor does not work. Increasing the temperature leads to the growth of fluctuations and the Brownian-motion-assisted nanomotor operation. The same tendencies can be seen in Fig. 5 showing the time-averaged torque as a function of the source-drain voltage.

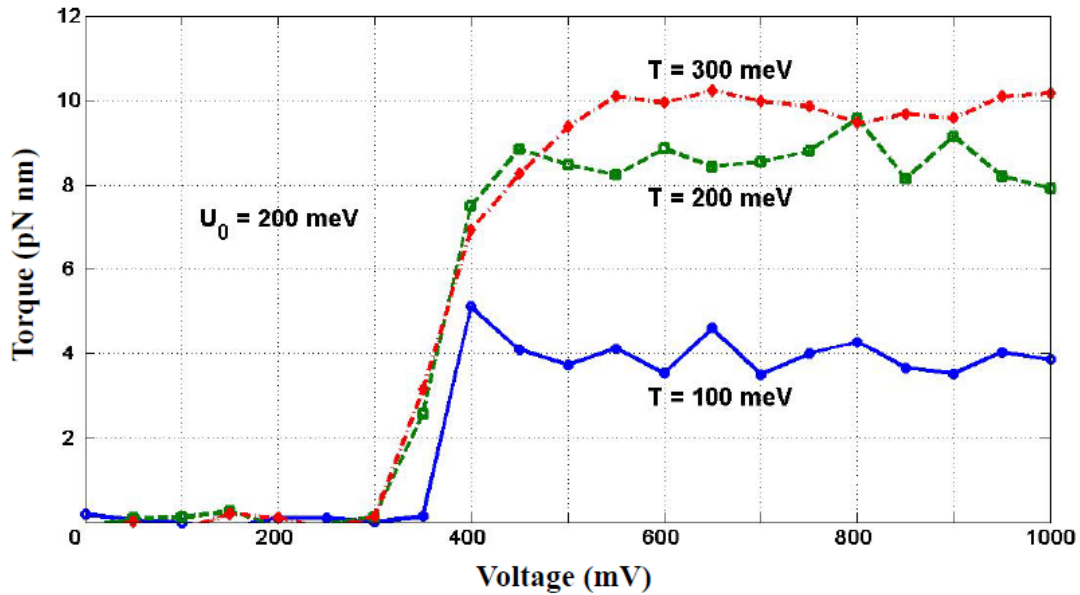


Fig. 5. Dependence of the time-averaged torque on the source-drain voltage.

We obtained the results above for the situation when no external torque is applied to the system. However, such torque can drastically affect the system behavior. In Fig. 6 we present the particle current as a function of the counterclockwise torque for various source-drain voltages applied to the nanomotor. Notice that the *dc* in-plane electric field is considerably larger in this case.

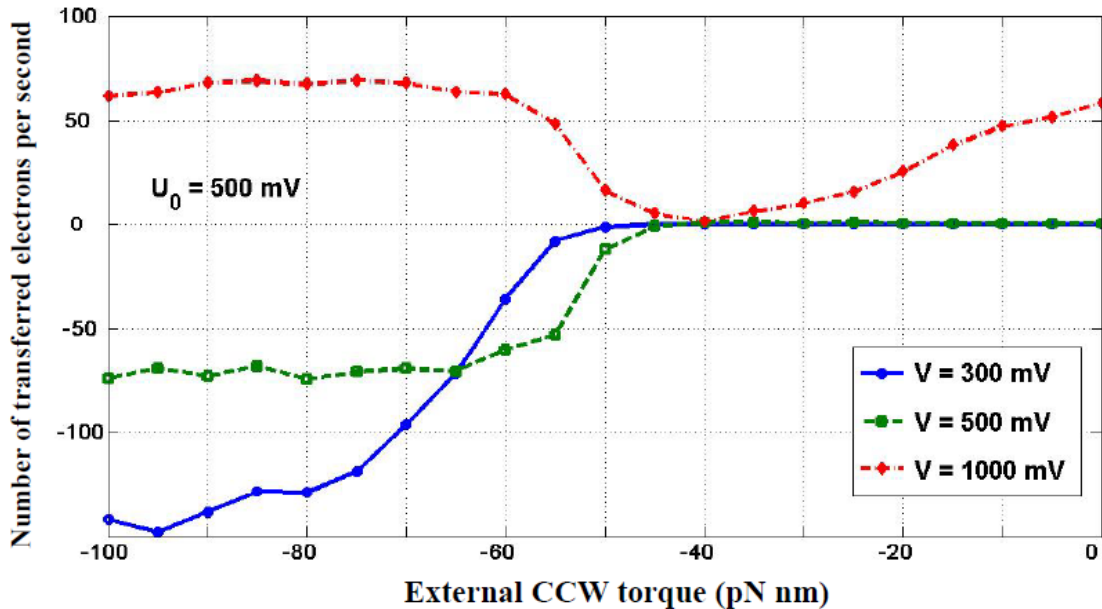


Fig. 6. Dependence of the particle current on the external counterclockwise (CCW) torque.

For relatively large but not significant values of the source-drain voltage and large enough external torque, the particle current is *negative* which means that electrons are transferred against the voltage, so the nanomotor works in the *pumping regime*. Only an applied voltage of the order of one volt can overcome this external torque.

The efficiency of the nanomotor can be described by the following expression

$$Eff = \frac{\langle N \rangle \langle \Omega \rangle}{IV}, \quad (9)$$

where  $\langle N \rangle$  and  $\langle \Omega \rangle$  are the averaged torque and angular velocity, respectively,  $I$  is the particle current and  $V$  is the applied voltage. For the parameters of our model this efficiency can be up to 85% which makes this nanomotor structure highly attractive for device purposes. The efficiency of real biological nanomotors can be up to 90%.

#### 4. CONCLUSIONS

In conclusion, we have examined a system of three quantum dots placed on a nanorotor in the presence of an external electric field. When the dots are connected to the source (drain) reservoirs, they are electron-populated (- depopulated) which induces a torque on the nanorotor and eventually leads to unidirectional rotation of the system. Using two source reservoirs coupled in different positions, the direction of rotation can be alternated. We have determined the dependencies of the time-averaged electron particle current and induced torque on the source-drain voltage, in-plane electric field strength, and temperature. We have also showed that the application of an external torque can lead to the operation of the system in the pumping regime with electrons transferred from the drain to the source against the applied voltage. The efficiency of such system can be up to 85% at room temperature.

#### ACKNOWLEDGEMENTS

This work was supported in part by the National Security Agency, Laboratory of Physical Science, Army Research Office, National Science Foundation Grant No. EIA-0130383, Contract No. JSPS-RFBR 06-02-91200, and Core-to-Core (CTC) program supported by the Japan Society for Promotion of Science (JSPS). S.S. acknowledges support from the EPSRC ARF Contract No. EP/D072581/1 and AQDJJ network programme. L.M. was partially supported by the NSF NIRT, Grant No. ECS-0609146.

#### REFERENCES

- [1] Alberts, B., Johnson, A., Lewis, J., Raff, M., Roberts, K., Walter, P., *Molecular Biology of the Cell* (Garland Science, New York, 2002), Ch. 11 and Ch. 14.
- [2] Browne, W. R., Feringa, B. L., "Making Molecular Machines Work", *Nature Nanotechn.* 1, 25 (2006).
- [3] Elston, T., Wang, H., Oster, G., "Energy transduction in ATP synthase", *Nature* 391, 510 (1998).
- [4] Dimroth, P., Wang, H., Grabe, M., Oster, G., "Energy transduction in the sodium F-ATPase of *Propionigenium modestum*", *Proc. Nat. Acad. Sci. USA* 96, 4924 (1999).
- [5] Oster, G., Wang, H., "Rotary protein motors", *Trends in Cell Biology* 13, 114 (2003).
- [6] Berg, H. C., "The rotary motor of bacterial flagella", *Annu. Rev. Biochem.* 72, 19 (2003).
- [7] Smirnov, A. Yu., Savel'ev, S., Mourokh L. G., Nori F., "Unidirectional rotary nanomotors powered by an electrochemical potential gradient," arxiv: cond-matt 0712.3310.
- [8] Smirnov, A. Yu., Savel'ev, S., Mourokh L. G., Nori F., "Proton transport and torque generation in rotary biomotors," *Phys. Rev. E* 78, 031921 (2008).
- [9] Wang, B., Vukovic, L., Kral, P., "Nanoscale rotary motors driven by electron tunneling," *Phys. Rev. Lett.* 101, 186808 (2008).
- [10] Wingreen, N. S., Jauho, A.-P., Meir, Y., "Time-dependent transport through a mesoscopic structure," *Phys. Rev. B* 48, 8487 (1993).
- [11] Mourokh, L. G., Horing, N. J. M., Smirnov, A. Yu., "Electron transport through a parallel double-dot system in the presence of Aharonov-Bohm flux and phonon scattering," *Phys. Rev. B* 66, 085332 (2002).